Nuclear Inst. and Methods in Physics Research, A 1029 (2022) 166473

Contents lists available at ScienceDirect

Nuclear Inst. and Methods in Physics Research, A

journal homepage: www.elsevier.com/locate/nima

Sensitivity and fading of irradiated RADFETs with different gate voltages

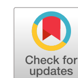

Goran S. Ristic [a,*], Stefan D. Ilic [a,f], Marko S. Andjelkovic [b], Russell Duane [c], Alberto J. Palma [d], Antonio M. Lalena [g], Milos D. Krstic [b,e], Aleksandar B. Jaksic [c]

[a] Faculty of Electronic Engineering, University of Niš, Niš, Serbia
[b] IHP - Leibniz-Institut für innovative Mikroelektronik, Frankfurt (Oder), Germany
[c] Tyndall National Institute, University College Cork, Cork, Ireland
[d] Department of Electronics and Computer Technology, University of Granada, Granada, Spain
[e] University of Potsdam, Potsdam, Germany
[f] Center of Microelectronic Technologies, Institute of Chemistry, Technology and Metallurgy, University of Belgrade, Serbia
[g] Department of Atomic, Molecular and Nuclear Physics, University of Granada, Granada, Spain

ARTICLE INFO

Keywords:
pMOS radiation dosimeter
RADFETs
Irradiation
Sensitivity
Annealing
Fading

ABSTRACT

The radiation-sensitive field-effect transistors (RADFETs) with an oxide thickness of 400 nm are irradiated with gate voltages of 2, 4 and 6 V, and without gate voltage. A detailed analysis of the mechanisms responsible for the creation of traps during irradiation is performed. The creation of the traps in the oxide, near and at the silicon/silicon-dioxide (Si/SiO_2) interface during irradiation is modelled very well. This modelling can also be used for other MOS transistors containing SiO_2. The behaviour of radiation traps during postirradiation annealing is analysed, and the corresponding functions for their modelling are obtained. The switching traps (STs) do not have significant influence on threshold voltage shift, and two radiation-induced trap types fit the fixed traps (FTs) very well. The fading does not depend on the positive gate voltage applied during irradiation, but it is twice lower in case there is no gate voltage. A new dosimetric parameter, called the Golden Ratio (GR), is proposed, which represents the ratio between the threshold voltage shift after irradiation and fading after spontaneous annealing. This parameter can be useful for comparing MOS dosimeters.

1. Introduction

The investigation of the influence of ionizing radiation on p-channel metal–oxide–semiconductor field-effect-transistors (pMOSFETs) with Al-gate, in order to use them as radiation sensors, has been widely conducted [1–8]. They can be used in medicine (radiotherapy) and space, but their application in personal dosimetry is still promising. In recent years, new technologies and materials have been used to produce new radiation-sensitive pMOSFETs, often called RADFETs or pMOS dosimeters [9–18]. Besides, the possibility of using commercial pMOSFETs as radiation detectors has been investigated [19,20].

During irradiation, traps are formed in the gate oxide, close to and exactly at the silicon/silicon-dioxide interface. These traps influence the carriers in the channel, which leads to an increase in threshold voltage. The two basic dosimetric parameters of RADFET are sensitivity (increase of threshold voltage during irradiation) and fading (recovery of threshold voltage of irradiated RADFETs during room temperature annealing without gate voltage). Radiation sensitivity should be as high as possible and fading as low as possible.

In this paper, the dependence of threshold voltage, which is the electrical and dosimetric parameter of RADFETs, on traps created during irradiation is investigated. Knowledge of the mechanisms that lead to the creation of traps under the influence of radiation is important for the operation of RADFETs, as well as other MOSFETs, and their analysis has been performed. In addition to irradiation, post-irradiation annealing was performed at room temperature without gate voltage (spontaneous annealing), and the dependence of the threshold voltage recovery during spontaneous annealing (fading) on the radiation-induced traps was analysed.

2. Experimental details

The used RADFETs have an oxide thickness of 400 nm and pre-irradiation threshold voltages of about V_{T0} = 1.9 V. Fig. 1 shows the cross section of RADFETs.

The irradiation of RADFETs was performed by a ^{60}Co source of ionizing radiation [21,22], using an absorbed dose rate of D_R = 7.69 Gy(H_2O)/h, and an absorbed dose of D = 110 Gy(H_2O). During the irradiation, the voltages at the gate were $V_{G,rad}$ = 0, 2, 4 and 6 V, while drain, source and bulk were grounded (in the case of $V_{G,rad}$ = 0 V, all pins were grounded). We have chosen relatively small voltages that can be applied in the practical realization of the radiation dosimeters. The experimental setup was composed of an ultra-low current, high

* Corresponding author.
E-mail address: goran.ristic@elfak.ni.ac.rs (G.S. Ristic).

https://doi.org/10.1016/j.nima.2022.166473
Received 16 May 2021; Received in revised form 29 September 2021; Accepted 23 January 2022
Available online 16 February 2022
0168-9002/© 2022 The Author(s). Published by Elsevier B.V. This is an open access article under the CC BY license (http://creativecommons.org/licenses/by/4.0/).

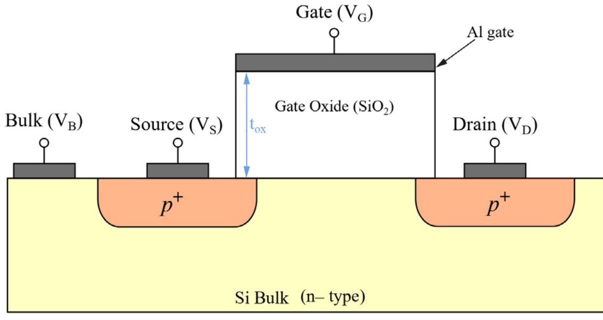

Fig. 1. Typical RADFET cross-section.

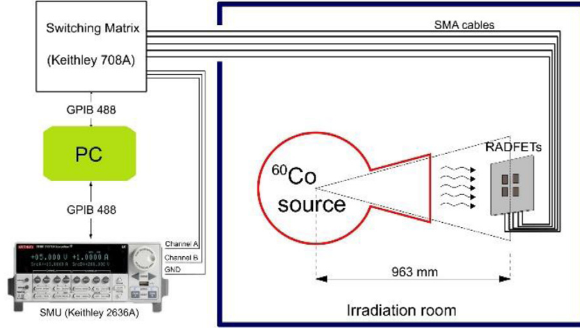

Fig. 2. The block diagram of experimental setup.

Table 1
Experimental conditions.

Label of used RADFET	t_{ox} (nm)	$V_{G,rad}$ (V)	$V_{G,sa}$ (V)
XW4 12	400	0	0
XW4 17	400	2	0
XW4 20	400	4	0
XW4 21	400	6	0

speed switching matrix model 708A Keithley, and a low current dual-channel source meter unit (SMU) model 2636A Keithley (Fig. 2). The experiment was guided by PC using a custom-written program in C#. Such configuration enabled completely automatic experiment, and the samples were neither moved nor touched during the irradiation, but the RADFETs were biased and their electrical characteristics were measured at certain times.

After the irradiation, RADFETs were spontaneous annealed, representing the room-temperature annealing without a gate voltage ($V_{G,sa}$ = 0 V – all pins were grounded), up to 1968 h. The experimental details are given in Table 1.

In cases of zero bias ($V_{G,rad}$ = 0 V and $V_{G,sa}$ = 0 V), there is a small external positive gate voltage of V_{wf} = 0.33 V for these RADFETs, as a consequence of the work function difference between the Al-gate and n-type silicon substrate [21]. This V_{wf} gives an external positive electric field of $E_{wf} = V_{wf}/t_{ox} \approx 0.825$ V/μm with direction from the gate to the oxide/substrate (SiO_2/Si) interface.

The threshold voltage before irradiation, V_{T0}, and during irradiation and spontaneous annealing, V_T, was determined by the electrical transfer characteristics in saturation [21]. The measurements of the electrical transfer characteristics of RADFETs were performed using an automatic system shown in Fig. 2. The threshold voltage shift, ΔV_T, is:

$$\Delta V_T = V_T - V_{T0}. \tag{1}$$

The midgap-subthreshold technique (MGT) that determines the component of the threshold voltage shift of fixed traps (FTs), ΔV_{ft}, and of switching traps (STs), ΔV_{st}, was used [23]. The ΔV_T during irradiation and annealing can be presented as:

$$\Delta V_T = \Delta V_{ft} + \Delta V_{st}. \tag{2}$$

Using the ΔV_{ft} and ΔV_{st}, the areal densities of FTs, ΔN_{ft} [cm^{-2}], and STs, ΔN_{st} [cm^{-2}] can be found [23]:

$$\Delta N_{ft} = \frac{C_{ox}}{e}\Delta V_{ft}, \qquad \Delta N_{st} = \frac{C_{ox}}{e}\Delta V_{st}. \tag{3}$$

where $C_{ox} = \varepsilon_{ox}/t_{ox}$ is the gate oxide capacitance per unit area, $\varepsilon_{ox} = 3.45 \cdot 10^{-13}$ F/cm is the silicon-dioxide permittivity, and e is the electron charge.

Since the MGT is an electrical measurement technique, which does not really recognize the physical location of the traps, but recognizes the electrical activity of created traps, we usually use the ΔN_{ft} and ΔN_{st}, as they really reflected the electrical response of the traps, than the more commonly used quantities that imply the physical location of the traps: the density of oxide traps (the traps in the oxide), ΔN_{ot}, and the density of interface states (the states exactly at SiO_2/Si interface), ΔN_{it}.

The traps created by any stress (radiation, electric fields, annealing, ...), which do not capture the carriers from channel (do not exchange carriers (charge) with channel) within the time frame of the electrical MG measurement, represent the FTs. The traps, created by any stress, which capture the carriers from channel (exchange carriers (charge) with channel) within the time frame of the electrical MG measurement represent the STs [24].

The STs consist of traps created in the oxide, but very near the SiO_2/Si interface, called the slow switching traps (SSTs) or border traps, and of traps created exactly at SiO_2/Si interface, called fast switching traps (FSTs), true interface traps (true interface states), or simply interface traps (states). The correlation between the densities of these traps is [21]:

$$\Delta N_{st} = \Delta N_{sst} + \Delta N_{fst}, \tag{4}$$

where ΔN_{sst} is the density of SSTs and ΔN_{fst} is the density of FSTs. It is obvious that ΔN_{ot} includes the FTs and SSTs, but ΔN_{it} only includes FSTs, and the correlations are: $\Delta N_{ot} = \Delta N_{ft} + \Delta N_{sst}$ and $\Delta N_{it} = \Delta N_{st} - \Delta N_{sst} = \Delta N_{fst}$.

3. Results and discussion

3.1. Radiation

The threshold voltage, V_T, during irradiation with different gate voltages, $V_{G,rad}$, is shown in Fig. 3. It is obvious that the $V_{G,rad}$ has a significant influence on V_T, and that the dependence of V_T = f($V_{G,rad}$) is not linear, but shows a saturation trend (see the last irradiation points). Figs. 3 and 4 show the components of ΔV_T of fixed traps (FTs), ΔV_{ft}, and switching traps (STs), ΔV_{st}. The ΔV_{ft} and Δ BXMATH[70] were found using MGT [23,24]. It can be seen that the density of FTs significantly depends on V_G, while V_G has no effect on the density of STs. Namely, the density of STs is approximately the same for all gate voltages, including irradiation case without gate voltage. Also, the density of FTs is at least five times higher than the density of STs, except for $V_{G,rad}$ = 0 V, where the densities of FTs and STs are approximately the same.

Knowledge of the mechanisms that lead to the formation of FTs and STs due to the irradiation is very important for all MOSFETs, including RADFETs [24–27] (see Fig. 5).

During ionizing irradiation, photons collide with electrons bound in the silicon-dioxide (SiO_2), mainly through Compton scattering, releasing bound electrons (so-called "primary" electrons) and leaving unoccupied electron sites (so-called holes). Since non-strained silicon–oxygen bonds (NSBs), $\equiv Si_o{-}O{-}Si_o\equiv$, are the most numerous bond in

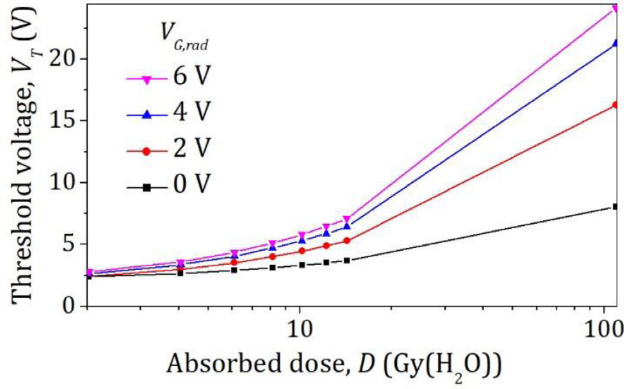

Fig. 3. Threshold voltage, V_T, during irradiation.

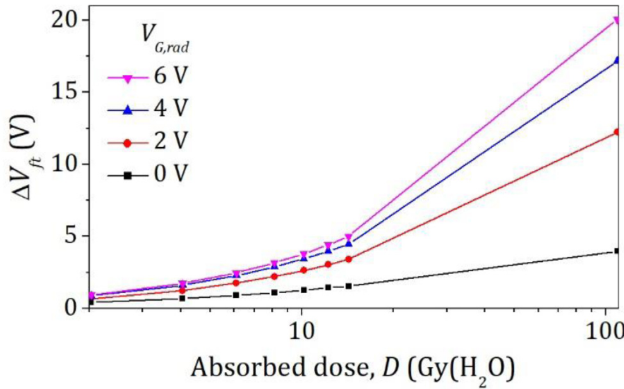

Fig. 4. The component of threshold voltage shift of fixed traps (FTs).

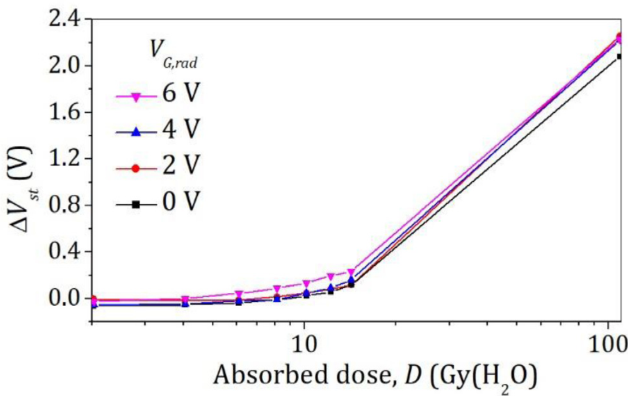

Fig. 5. The component of threshold voltage shift of switching traps (STs).

SiO_2, collisions between photons and electrons in NSBs are most likely [24]:

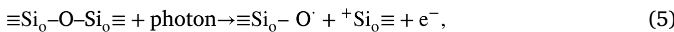

$$\equiv Si_o\text{–}O\text{–}Si_o\equiv + \text{photon} \rightarrow \equiv Si_o\text{– }O^{\cdot} + {}^{+}Si_o\equiv + e^{-}, \tag{5}$$

where the index "o" denotes oxide, but "–" denotes covalent bond (a pair of electrons). An unpaired electron e^- is usually at the $\equiv Si_o\text{-}O^{\cdot}$ centre (e^- is denoted by a dot), but a hole h^+ (positively charged virtual particle) is at ${}^{+}Si_o\equiv$ centre (h^+ is denoted by a plus sign).

Primary electrons have very high kinetic energy, and either recombine with holes at the site of formation or avoid recombination. Due to their high kinetic energy, recombination is a very low probable process. The primary electrons, avoiding recombination, travel through the oxide and collide with the bound electrons in the covalent bonds of the NSBs. In these collisions, they lose kinetic energy and release so-called "secondary" electrons [24]:

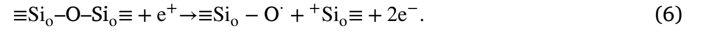

$$\equiv Si_o\text{–}O\text{–}Si_o\equiv + e^{+} \rightarrow \equiv Si_o - O^{\cdot} + {}^{+}Si_o\equiv + 2e^{-}. \tag{6}$$

Collisions between free electrons are hardly probable because their cross section is significantly smaller than the cross section of NSBs.

Primary and secondary electrons, before leaving the oxide, break many covalent bonds in the oxide and create many new high-energy secondary electrons because they have very high kinetic energies [24]. Otherwise, the primary and secondary electrons, moving freely through the oxide, break many more covalent bonds than incident photons of ionizing radiation.

Electrons leave the oxide very quickly (in a few picoseconds), while the holes remain trapped. Holes in the bulk of the oxide are usually only temporary, but not permanently trapped at the point of origin (reactions (5) and (6)), because there are no deeper energy centres in the oxide bulk [24]. However, the holes move towards an interface, depending on the oxide electric field's direction, where they are trapped in the energy-deep hole centres.

In zero bias mode, the small positive potential, due to the difference in work function between the *Al*-gate and the n-substrate, is high enough to move at least part of the holes towards the SiO_2/Si interface [22]. It is unlikely that electrons will be trapped at electron trapping centres in the case of irradiation [24].

In the area of 3–5 nm from the SiO_2/Si interface, there are a lot of both the oxygen vacancies (OVs), $\equiv Si_o\text{–}Si_o\equiv$, and the strained silicon–oxygen bonds (SBs), $\equiv Si_o\text{–}O\text{–}Si_o\equiv$ [24]. The OVs and SBs are the main precursors of fixed traps (FTs) whose density ΔN_{ft} can be found by the MG technique.

When the holes, under a positive electric field, reach the area near SiO_2/Si interface, they break the OVs, $\equiv Si_o\text{–}Si_o\equiv$ [24]:

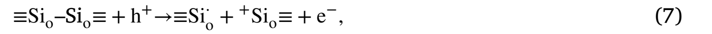

$$\equiv Si_o\text{–}Si_o\equiv + h^{+} \rightarrow \equiv Si_o^{\cdot} + {}^{+}Si_o\equiv + e^{-}, \tag{7}$$

where the ${}^{+}Si_o\equiv$ centre is named as the E_γ centre, and also break the SBs, $\equiv Si_o\text{–}O\text{–}Si_o\equiv$ [24]:

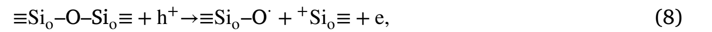

$$\equiv Si_o\text{–}O\text{–}Si_o\equiv + h^{+} \rightarrow \equiv Si_o\text{–}O^{\cdot} + {}^{+}Si_o\equiv + e, \tag{8}$$

where the $\equiv Sio\text{–}O^{\cdot}$ is an amphoteric non-bridging-oxygen (NBO) centre, while ${}^{+}Si_o\equiv$ is the E_s centre. E_γ and E_s represent energetically deep hole centres.

The NBO is an amphoteric defect and can be positively or negatively charged. However, they are more likely to be negatively charged by electron capture than to be positively charged by electron release. As already mentioned, these processes are not so likely during irradiation.

By Eq. (7), the kinetic of the OVs centres can be presented as:

$$-\frac{d[N_{ov,ft}]}{dt} = k_{ov,ft}[N_{ov,ft}][h^{+}], \tag{9}$$

where $[N_{ov,ft}]$ is the density of OVs, $k_{ov,ft}$ is the constant and $[h^+]$ is the hole density. The $[N_{ov,ft}]$ density decreases with the irradiation time, i.e., with absorbed dose, how OV bonds are broken (it indicates minus).

By solving Eq. (9), we obtained the dependence of the density of OVs on the irradiation time *t*, $N_{ov,ft}(t)$:

$$N_{ov,ft}(t) = N_{ov,ft}(0) \cdot e^{-k_{ov,ft} \cdot t}, \tag{10}$$

where the $N_{ov,ft}(0)$ is the density of OVs for $D = 0$. During irradiation, while $N_{ov,ft}(t)$ decreases, the density of positively charged centres ${}^{+}Si_o\equiv$ (E_γ centres), created by radiation, $\Delta N_{ov,ft}(t)$, increases:

$$\Delta N_{ov,ft}(t) = N_{ov,ft}(0)(1 - e^{-k_{ov,ft} \cdot t}). \tag{11}$$

Similarly, Eq. (8) gives:

$$-\frac{d[N_{sb,ft}]}{dt} = k_{sb,ft}[N_{sb,ft}][h^{+}], \tag{12}$$

where $[N_{sb,ft}]$ is the density of SBs, $k_{sb,ft}$ is the constant and $[h^+]$ is the hole density. The $[N_{sb,ft}]$ density decreases with absorbed dose (it indicates minus).

Solving Eq. (12) gives the density of SBs with the irradiation time, $N_{sb,ft}(t)$:

$$N_{sb,ft}(t) = N_{sb,ft}(0) \cdot e^{-k_{sb,ft} \cdot t}, \tag{13}$$

where the $N_{sb,ft}(0)$ is the density for $D = 0$. During irradiation, while the $N_{sb,ft}(t)$ decreases, the density of positively charged centres $^+Si_o\equiv$ (E_s centres), created by radiation, $\Delta N_{sb,ft}(t)$, increases:

$$\Delta N_{sb,ft}(t) = N_{sb,ft}(0)(1 - e^{-k_{sb,ft} \cdot t}). \tag{14}$$

The relation between absorbed dose, D, and absorbed dose rate, D_R ($D = D_R \cdot t$), gives the dependence of absorbed dose:

$$\Delta N_{ov,ft}(D) = N_{ov,ft}(0)(1 - e^{-a_{ov,ft} D}), \tag{15}$$

where the $a_{ov,ft} = k_{ov,ft}/D_R$, but $k_{ov,ft}$ and D_R are constants. Also,

$$\Delta N_{sb,ft}(D) = N_{sb,ft}(0)(1 - e^{-a_{sb,ft} D}), \tag{16}$$

where the $a_{sb,ft} = k_{sb,ft}/D_R$.

Obviously, the following relation exists: $\Delta N_{ft}(D) = \Delta N_{ov,ft}(D) + \Delta N_{sb,ft}(D)$. Using Eq. (3), we got:

$$\Delta V_{ft}(D) = \Delta V_{ov,ft}(D) + \Delta V_{sb,ft}(D), \tag{17}$$

$$\Delta V_{ov,ft}(D) = V_{ov,ft}(1 - e^{-a_{ov,ft} D}), \tag{18}$$

$$\Delta V_{sb,ft}(D) = V_{sb,ft}(1 - e^{-a_{sb,ft} D}). \tag{19}$$

The used MG technique also determines the density of switching traps (STs), ΔN_{st}. The STs contain [24]: the slow switching traps (SSTs), located near the SiO_2/Si interface, whose density is ΔN_{sst}, and fast switching traps (FSTs), located exactly on this interface, whose density is ΔN_{fst}. The relation between these densities is given by Eq. (4), but the component of threshold voltage shift induced by the STs, ΔV_{st}, is:

$$\Delta V_{st}(D) = \Delta V_{sst}(D) + \Delta V_{fst}(D), \tag{20}$$

where the ΔV_{sst} and ΔV_{fst} represent contributions of SSTs and FSTs, respectively.

The OVs and SBs also exist near SiO_2/Si interface and the same methodology can be applied to SSTs, as it was applied to FTs. This procedure gives an equation similar with Eqs. (17)–(19):

$$\Delta V_{sst}(D) = V_{ov,sst}(1 - e^{-a_{ov,sst} D}) + V_{sb,sst}(1 - e^{-a_{sb,sst} D}). \tag{21}$$

The contribution of FSTs, ΔV_{fst}, to ΔV_{st} during irradiation can usually be neglected, giving: $\Delta V_{st}(D) \approx \Delta V_{sst}(D)$.

Fig. 6 represents the experimental values of ΔV_T, ΔV_{ft}, and ΔV_{st} during irradiation with $V_{G,rad} = 4$ V, as well as the fitting of ΔV_{ft} and ΔV_{st} using Eqs. (17) and (21), respectively, but ΔV_T was obtained using Eq. (2). For all gate voltages, the fitting is very well (no results for other voltages are shown). All fittings were performed using the GUI Octave 6.2.0 program.

However, this fitting procedure of $\Delta V_T(D)$ is complicated for dosimetric purposes. Therefore, our idea is to use a simple function that would fit $\Delta V_T(D)$ well. Our investigations have shown that $\Delta V_T(D)$ can be fitted very well using the equation proposed in [21,22]:

$$\Delta V_T(D) = \Delta V_{T,sat} - \frac{\Delta V_{T,sat}}{1 + bD^c} \tag{22}$$

where $\Delta V_{T,sat}$, b and c are the positive constants. The $\Delta V_{T,sat}$ represents the saturation value of $\Delta V_T(D)$ and can be used to find the dependence of $\Delta V_T(D)$ on $V_{G,rad}$.

Fig. 7 shows that the fit of $\Delta V_T(D)$ using Eq. (22) is very well. We obtained a much better fit using Eq. (22) than using power-law function: $\Delta V_T(D) = a \cdot D^b$, and exponential function: $\Delta V_T(D) = a(1 - exp(-b \cdot D))$, where a and b are positive constants. An important characteristic of Eq. (22) that it saturates for $D \to \infty$. Yilmaz et al. [1] and Kahraman et al. [16] also used Eq. (22) and obtained a very well fit of ΔV_T. The values of $\Delta V_{T,sa}$, b and c are given in Table 2.

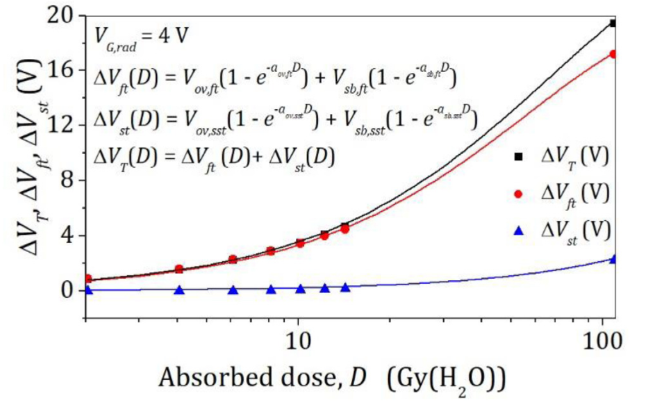

Fig. 6. Fitting of ΔV_{ft} and ΔV_{st} during irradiation by Eqs. (17) and (21).

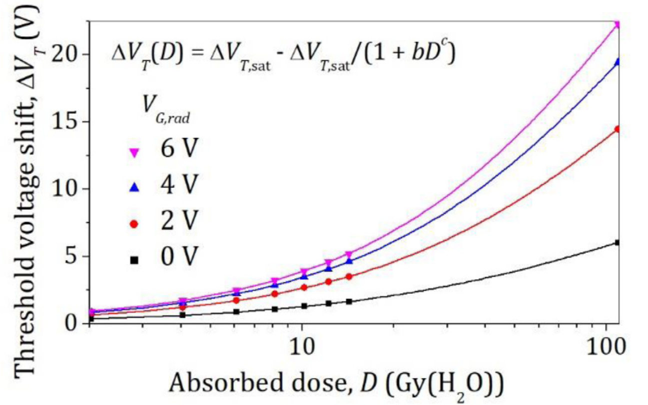

Fig. 7. Fitting of ΔV_T dependence on dose by Eq. (22).

Table 2
The parameters $\Delta V_{T,sat}$, b and c of the fitting shown in Fig. 7.

$V_{G,rad}$ (V)	$\Delta V_{T,sat}$ (V)	b (Gy^{-1})	c
0	14.759	0.0137	0.836
2	35.511	0.0100	0.901
4	44.935	0.0098	0.928
6	52.073	0.0093	0.935

3.2. Spontaneous annealing

The room-temperature annealing (RTA) without gate voltage ($V_{G,rta} = 0$ V) of irradiated RADFETs is known as spontaneous annealing (SA) [28–31].

During the annealing with zero or positive gate voltage, electrons tunnel from the substrate (Si) to the gate oxide (SiO_2) due to a positive electric field, where they compensate or/and neutralize the E_γ and E_s traps:

$$\equiv Si_o^{+\cdot} Si_o\equiv + e^- \rightarrow \equiv Si_o^{\cdot\cdot} \, ^{\cdot}Si_o\equiv, \tag{23}$$

$$\equiv Si_o^{+\cdot} O\text{–}Si_o\equiv + e^- \rightarrow \equiv Si_o^{\cdot\cdot} \, ^{\cdot}O\text{–}Si_o\equiv. \tag{24}$$

Using Eqs. (23) and (24), we obtained the dependence of densities of E_γ, $\Delta N_{E_\gamma}(t)$, and E_s, $\Delta N_{E_s}(t)$, on time during SA:

$$-\frac{d[N_{E_\gamma}]}{dt} = k_\gamma [N_{E_\gamma}][e^-] \Rightarrow \Delta N_{E_\gamma}(t) = \Delta N_{E_\gamma}(0) e^{-t/\tau_\gamma} \tag{25}$$

$$-\frac{d[N_{E_s}]}{dt} = k_s [N_{E_s}][e^-] \Rightarrow \Delta N_{E_s}(t) = \Delta N_{E_s}(0) e^{-t/\tau_s} \tag{26}$$

where $\Delta N_{E_\gamma}(0)$ and $\Delta N_{E_s}(0)$ are the densities of E_γ and E_s after irradiation, respectively, but $\tau_\gamma = 1/k_\gamma$ and $\tau_s = 1/k_s$ are the constants that show annealing rates. Obviously, on the basis of the above discussion, we can write:

$$\Delta N_{ft}(t) = \Delta N_{E_\gamma}(t) + \Delta N_{E_s}(t), \tag{27}$$

$$\Delta V_{ft}(t) = \Delta V_{E_\gamma}(t) + \Delta V_{E_s}(t), \tag{28}$$

$$\Delta V_{ft}(t) = V_\gamma e^{-t/\tau_\gamma} + V_s e^{-t/\tau_s}. \tag{29}$$

Since our experimental results show a slight increase in ΔN_{st} during annealing, we assume that this can be attributed to the FSTs. The formation of FSTs is probably performed by the hydrogen ions, H^+ [24]. The holes h^+ react with $\equiv Si_o$–H and $\equiv Si_o$–OH defects in the oxide and release H^+ ions that move to the interface because there is a positive electric field. At the interface, H^+ ions react with electrons that tunnel from silicon to oxide, and form hydrogen atoms, H^o. Then, FSTs are created in the following reaction at the SiO_2/Si interface:

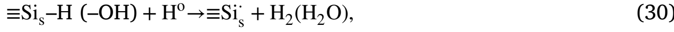

$$\equiv Si_s\text{–H (–OH)} + H^o \rightarrow \equiv Si_s^{\cdot} + H_2(H_2O), \tag{30}$$

where $\equiv Si_s^{\cdot}$ centre is the P_b centre.

Using Eq. (30) and the previous procedure, we obtained the equation for density of $\equiv Si_s$–H (–OH) defects during annealing, N_H(t):

$$-\frac{d[N_H]}{dt} = k_H[N_H][H^o] \Rightarrow N_H(t) = N_H(0)e^{-k_H \cdot t}, \tag{31}$$

where the $N_H(0)$ is the density of $\equiv Si_s$–H (–OH) defects at the beginning of annealing, $[H^o]$ is the hydrogen atom density and k_H is the reaction rate constant. During annealing, while the $N_H(t)$ decreases, the density of P_b ($\equiv Si_s^{\cdot}$) centres, $\Delta N_H(t)$, increases:

$$\Delta N_H(t) = N_H(0) - N_H(0)e^{-k_H t}. \tag{32}$$

The P_b centres are FSTs, i.e., $\Delta N_{fst}(t) \equiv \Delta N_H(t)$, giving:

$$\Delta V_{st}(t) \equiv \Delta V_{fst}(t) = V_{fst}(1 - e^{-k_H t}). \tag{33}$$

Fig. 8 shows the fitting of ΔV_T, ΔV_{ft}, and ΔV_{st} during SA of irradiated RADFET with $V_{G,rad}$ = 4 V. A very good fit of the experimental results can be seen. Similar results were obtained for other gate voltages $V_{G,rad}$ (not shown). The STs have a negligible effect on ΔV_T, and ΔV_T can be modelled by including only FTs. It should be noted that the ΔV_{st} is about seven times less than the ΔV_{ft} at the beginning of SA (about eight times at the end of irradiation — see Fig. 6). The results in Fig. 4 show that FTs, and thus ΔV_T, can be very successfully modelled during SA using two types of radiation-induced FTs (Eq. (29)). This fitting procedure is complicated for dosimetric purposes, but it is a very important for physical mechanisms investigation in RADFETs, as well as in other MOSFETs, during thermal and room-temperature annealing.

The threshold voltage shifts during SA, ΔV_T, of irradiated RADFETs with different positive gate voltages, $V_{G,rad}$, are shown in Fig. 9. The $V_{G,rad}$ obviously influences ΔV_T, but a dependence ΔV_T = f($V_{G,rad}$) displayed in this graph is not suitable for bringing some conclusions about both the level of recovering and dependence of ΔV_T on $V_{G,rad}$.

Because of that, the fading, f, should be used [28,29]:

$$f = \frac{V_T(0) - V_{T,sa}(t)}{V_T(0) - V_{T0}} \tag{34}$$

where $V_T(0)$ is the threshold voltage after irradiation, i.e. at the beginning of SA, $V_T(t)$ is the threshold voltage during SA, and V_{T0} is the threshold voltage before irradiation.

On the basis of previous analysis, it is obvious that several mechanisms are included in fading behaviour, and its fitting by these mechanisms would be very complicated. However, the fading, as a dosimetric parameter, needs a simple fitting function.

Our investigations have shown that the following simple function can fit the fading f well [32]:

$$f = f_{sat} - \frac{f_{sat}}{1 + dt^e}, \tag{35}$$

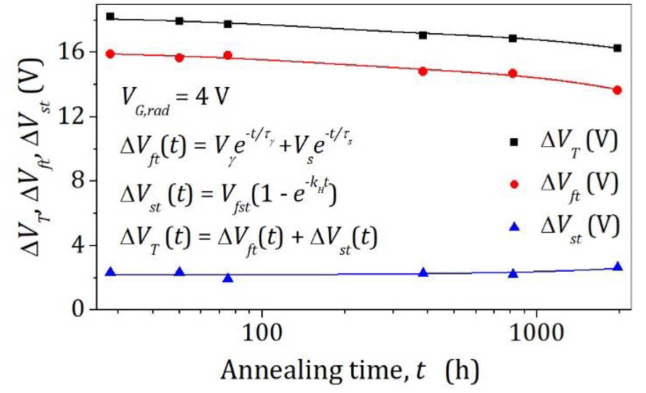

Fig. 8. Fitting of dependencies of ΔV_{ft} and ΔV_{st} on time by Eqs. (29) and (33).

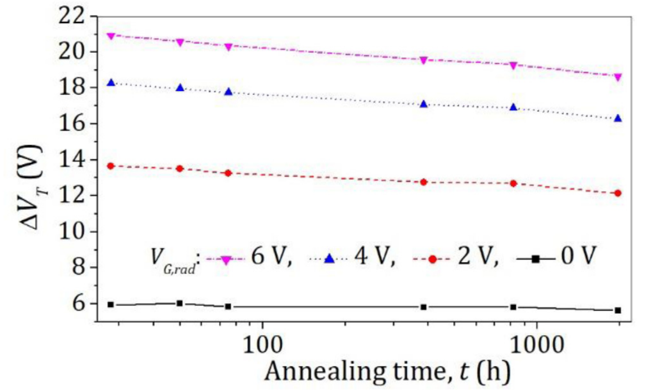

Fig. 9. The threshold voltages shift, ΔV_T, during SA of RADFETs irradiated with various gate voltages, $V_{G,rad}$.

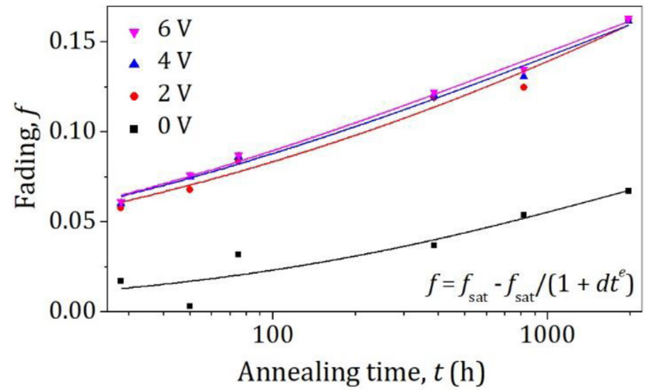

Fig. 10. The fading, f, of irradiated RADFETs with various gate voltages, $V_{G,rad}$, fitted by Eq. (35).

where t is the annealing time, f_{sat} is the saturation value of the fading, d and e are the positive constants. The results of fading and its fitting is shown in Fig. 10. The fading has almost the same values for all gate voltages applied during irradiation, except for $V_{G,rad}$ = 0 V, when fading is more than twice lower, and is well fitted by Eq. (35).

Fig. 11 represents the behaviours of ΔV_{ft} and ΔV_{st} during SA of irradiated RADFET with $V_{G,rad}$ = 0 V. The densities of FTs and STs show the opposite behaviour: the FT density decreases, while the ST density increases. On the basis of Eq. (34), it can be written [32]:

$$f = \frac{\Delta V_T(0) - \Delta V_{T,sa}(t)}{\Delta V_T(0)} = \frac{\Delta V_T(0) - (\Delta V_{ft,sa}(t) + \Delta V_{st,sa}(t))}{\Delta V_T(0)} \tag{36}$$

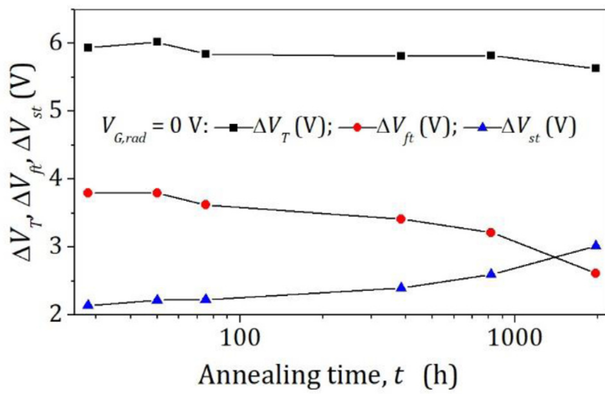

Fig. 11. The ΔV_T, ΔV_{ft} and ΔV_{st} during SA ($V_{G,rad}$, = 0 V).

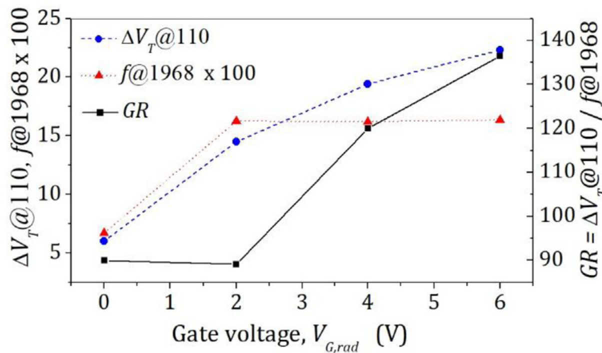

Fig. 12. The dependence of ΔV_T@110, f@1968 and GR on gate voltage.

where $\Delta V_T(0)$ is the threshold voltage shift after irradiation, i.e. at the beginning of SA, and $\Delta V_{T,sa}(t)$ is the threshold voltage shift during SA. At beginning of SA (t = 0), $\Delta V_{T,sa}(0) = \Delta V_T(0)$, and f = 0. During SA, $\Delta V_{T,sa}(t)$ usually decreases, which gives the positive fading that increases. Else, $\Delta V_{T,sa}(t)$ can also increase (reverse annealing), giving the negative fading which absolute value increases. In Fig. 11, the decrease of FT density is somewhat higher than the increase of ST density, which leads to the decrease of $\Delta V_{T,sa}(t)$ (Eq. (2)), and the increase of positive fading (see Fig. 10).

Since the sensitivity and fading are sole dosimetric parameters, we can introduce a new dosimetric parameter, *Golden Ratio*, *GR*, that connects these two parameters:

$$GR = \frac{\Delta V_T(D_{\max})}{f(t_{\max})}, \tag{37}$$

where the $\Delta V_T(D_{max})$ is the ΔV_T at the last point of irradiation of 110 Gy and $f(t_{max})$ is the fading at the last point of SA of 1968 h. The higher *GR* represents the better dosimetric characteristics of the pMOS dosimeter that should have a large ΔV_T and a small *f*. This means that *GR* can be used as a good parameter to compare different pMOS dosimeters or to examine the effect of operating conditions (e.g. as in our case, different gate voltages).

The ΔV_T@110, f@1968 and *GR* are shown in Fig. 12. The f@1968 is multiplied by 100 so that it can be displayed on the same axis with ΔV_T@110. As can be seen, the highest *GR* (the best dosimetric characteristic) is for $V_{G,rad}$ = 6 V, and the smallest *GR* (the worst dosimetric characteristic) is for $V_{G,rad}$ = 2 V.

4. Conclusion

The experimental results show a non-linear increase in threshold voltage shift, ΔV_T, of used RADFETs during the irradiation up to 110 Gy. The dependence of ΔV_T on gate voltage, $V_{G,rad}$, applied during radiation is also not linear and has a saturation trend. Using the traps created by irradiation, dependence of threshold voltage shift on dose, $\Delta V_T = f(D)$, is modelled very well. This procedure can also be used for modelling of irradiation traps in various MOSFETs. However, this procedure is so complicated for dosimetric purposes, which need fast measurements. Because of that, the simple function for ΔV_T fitting, previously proposed, is used, and it fits ΔV_T very well. The ΔV_T during spontaneous annealing is modelled very well using the traps created during irradiation. Fading is also very well fitted with the previously proposed function. A potentially important dosimetric parameter (*Golden Ratio*, *GR*) is proposed. This parameter can be useful for comparing the different types of MOS dosimeters under the same conditions during radiation and annealing (voltage, temperature, …) or for comparing the one type of MOS dosimeter under different conditions. Here, based on *GR*, the best dosimetric characteristic has $V_{G,rad}$ = 6 V case.

CRediT authorship contribution statement

Goran S. Ristic: Writing – original draft, Writing – review & editing, Conceptualization, Investigation, Validation, Project administration. **Stefan D. Ilic:** Investigation, Software, Validation. **Marko S. Andjelkovic:** Conceptualization, Validation. **Russell Duane:** Conceptualization, Validation. **Alberto J. Palma:** Conceptualization, Validation. **Antonio M. Lalena:** Conceptualization, Validation. **Milos D. Krstic:** Conceptualization, Validation. **Aleksandar B. Jaksic:** Conceptualization, Validation.

Declaration of competing interest

The authors declare that they have no known competing financial interests or personal relationships that could have appeared to influence the work reported in this paper.

Acknowledgement

This work was supported in part by the European Union's Horizon 2020 research and innovation programme under grant agreement No. 857558, and the Ministry of Education, Science and Technological Development of the Republic of Serbia, under the project No. 43011.

References

[1] E. Yilmaz, A. Kahraman, A.M. McGarrigle, N. Vasovic, D. Yegen, A. Jaksic, Investigation of RadFET response to X-ray and electron beams, Appl. Radiat. Isot. 127 (2009) 156–160, http://dx.doi.org/10.1016/j.apradiso.2017.06.004.

[2] I. Mateu, M. Glaser, G. Gorine, M. Moll, G. Pezzullo, F. Ravotti, ReadMON: A portable readout system for the CERN PH-RADMON sensors, IEEE Trans. Nucl. Sci. 65 (2018) 1700–1707, http://dx.doi.org/10.1109/TNS.2017.2784684.

[3] M. Kulhar, K. Dhoot, A. Pandya, Gamma dose rate measurement using RadFET, IEEE Trans. Nucl. Sci. 66 (2019) 2220–2228, http://dx.doi.org/10.1109/TNS.2019.2942955.

[4] D.V. Andreev, G.G. Bondarenko, V.V. Andreev, A.A. Stolyarov, Use of high-field electron injection into dielectrics to enhance functional capabilities of radiation MOS sensors, Sensors 20 (2020) http://dx.doi.org/10.3390/s20082382, 2382–1–11.

[5] G. Biasi, F.-Y. Su, T. Al Sudani, S. Corde, M. Petasecca, M.L.F. Lerch, V.L. Perevertaylo, M. Jackson, A.B. Rosenfeld, On the combined effect of silicon oxide thickness and boron implantation under the gate in MOSFET dosimeters, IEEE Trans. Nucl. Sci. 67 (2020) 534–540, http://dx.doi.org/10.1109/TNS.2020.2971977.

[6] S. Carbonetto, M. Echarri, J. Lipovetzky, M. Garcia-Inza, A. Faigón, Temperature-compensated MOS dosimeter fully integrated in a high-voltage 0.35 μm CMOS process, IEEE Trans. Nucl. Sci. 67 (2020) 1118–1124, http://dx.doi.org/10.1109/TNS.2020.2966567.

[7] A.B. Rosenfeld, G. Biasi, M. Petasecca, M.L.F. Lerch, G. Villani, V. Feygelman, Semiconductor dosimetry in modern external-beam radiation therapy, Phys. Med. Biol. 65 (2020) 16TR01, http://dx.doi.org/10.1088/1361-6560/aba163.

[8] J.M. Sampaio, P. Goncalves, M. Pinto, J. Silva, V. Negîrneac, L. Sintra, C. Pinto, T. Sousa, P. Ribeiro, C. Poivey, Dose measurements and simulations of the RADFETs response onboard the Alphasat CTTB experiments, IEEE Trans. Nucl. Sci. 67 (2020) 2028–2033, http://dx.doi.org/10.1109/TNS.2020.3013035.

[9] H. Liu, Y. Yang, J. Zhang, A metal–oxide–semiconductor radiation dosimeter with a thick and defect-rich oxide layer, J. Micromech. Microeng. 26 (2016) http://dx.doi.org/10.1088/0960-1317/26/4/045014, 045014–1–7.

[10] S. Lai, P. Cosseddu, L. Basiricò, A. Ciavatti, B. Fraboni, A. Bonfiglio, A highly sensitive, direct X-ray detector based on a low-voltage organic field-effect transistor, Adv. Electron. Mater. 3 (2017) http://dx.doi.org/10.1002/aelm.201600409, 1600409–1–7.

[11] K.K. Lee, D. Wang, O. Shinobu, T. Ohshima, Reliability of gamma-irradiated n-channel ZnO thin-film transistors: Electronic and interface properties, Radiat. Eff. Defects Solids 173 (2018) 250–260, http://dx.doi.org/10.1080/10420150.2018.1427093.

[12] T. Cramer, I. Fratelli, P. Barquinha, A. Santa, C. Fernandes, F. D'Annunzio, C. Loussert, R. Martins, E. Fortunato, B. Fraboni, Passive radiofrequency x-ray dosimeter tag based on flexible radiation-sensitive oxide field-effect transistor, Sci. Adv. 4 (2018) http://dx.doi.org/10.1126/sciadv.aat1825, eaat1825–1–7.

[13] S. Jain, S.G. Surya, P.K. Suggisetti, A. Gupta, V.R. Rao, Sensitivity improvement of medical dosimeters using solution processed TIPS-Pentacene FETs, IEEE Sens. J. 19 (2019) 4428–4434, http://dx.doi.org/10.1109/JSEN.2019.2901810.

[14] S.A. Hadi, K.M. Humood, M.A. Jaoude, H. Abunahla, H.F. Al Shehhi, B. Mohammad, Bipolar Cu/HfO_2/p^{++} Si memristors by sol–gel spin coating method and their application to environmental sensing, Sci. Rep. 9 (2019) http://dx.doi.org/10.1038/s41598-019-46443-x, 9983–1–15.

[15] S. Jain, A.S. Gajarushi, A. Gupta, V.R. Rao, A passive gamma radiation dosimeter using graphene field effect transistor, IEEE Sens. J. 20 (2020) 2938–2944, http://dx.doi.org/10.1109/JSEN.2019.2958143.

[16] A. Kahraman, S.C. Deevi, E. Yilmaz, Influence of frequency and gamma irradiation on the electrical characteristics of Er_2O_3, Gd_2O_3, Yb_2O_3, and HfO_2 MOS-based devices, J. Mater. Sci. 55 (2020) 7999–8040, http://dx.doi.org/10.1007/s10853-020-04531-8.

[17] K. Tamersit, Performance assessment of a new radiation dosimeter based on carbon nanotube field-effect transistor: A quantum simulation study, IEEE Sens. J. 19 (2019) 3314–3321, http://dx.doi.org/10.1109/JSEN.2019.2894440.

[18] A.M. Zeidell, T. Ren, D.S. Filston, H.F. Iqbal, E. Holland, J.D. Bourland, J.E. Anthony, O.D. Jurchescu, Organic field-effect transistors as flexible, tissue-equivalent radiation dosimeters in medical applications, Adv. Sci. 7 (2020) http://dx.doi.org/10.1002/advs.202001522, 2001522–1–9.

[19] M.A. Carvajal, P. Escobedo, M. Jiménez-Melguizo, M.S. Martínez-García, F. Martínez-Martí, A. Martínez-Olmos, A.J. Palma, A compact dosimetric system for MOSFETs based on passive NFC tag and smartphone, Sensors Actuators A 267 (2017) 82–89, http://dx.doi.org/10.1016/j.sna.2017.10.015.

[20] H.A. Farroh, A. Nasr, K.A. Sharshar, A study of the performance of an n-channel MOSFET under gamma radiation as a dosimeter, J. Electron. Mater. 49 (2020) 5762–5772, http://dx.doi.org/10.1007/s11664-020-08330-4.

[21] G.S. Ristic, M.S. Andjelkovic, A.B. Jaksic, The behavior of fixed and switching oxide traps of RADFETs during irradiation up to high absorbed doses, Appl. Radiat. Isot. 102 (2015) 29–34, http://dx.doi.org/10.1016/j.apradiso.2015.04.009.

[22] G.S. Ristić, N.D. Vasović, M. Kovačević, A.B. Jakšić, The sensitivity of 100 nm RADFETs with zero gate bias up to dose of 230 Gy(si), Nucl. Instrum. Methods Phys. Res. B 269 (2011) 2703–2708, http://dx.doi.org/10.1016/j.nimb.2011.08.015.

[23] P.J. McWhorter, P.S. Winokur, Simple technique for separating the effects of interface traps and trapped-oxide charge in metal–oxide–semiconductor transistors, Appl. Phys. Lett. 48 (1986) 133–135, http://dx.doi.org/10.1063/1.96974.

[24] G.S. Ristic, Influence of ionizing radiation and hot carrier injection on metal–oxide–semiconductor transistors, J. Phys. D: Appl. Phys. 41 (2008) http://dx.doi.org/10.1088/0022-3727/41/2/023001, TR023001–1–19.

[25] O.V. Aleksandrov, On the effect of bias on the behavior of MOS structures subjected to ionizing radiation, Semiconductors 49 (2015) 774–779, http://dx.doi.org/10.1134/S1063782615060020.

[26] A. Dubey, A. Singh, R. Narang, M. Saxena, M. Gupta, Modeling and simulation of junctionless double gate radiation sensitive FET (RADFET) dosimeter, IEEE Trans. Nanotechnol. 17 (2018) 49–55, http://dx.doi.org/10.1109/TNANO.2017.2719286.

[27] Y. Abe, T. Umeda, M. Okamoto, S. Harada, Y. Yamazaki, T. Ohshima, The effect of γ-ray irradiation on optical properties of single photon sources in 4H-SiC MOSFET, Mater. Sci. Forum 1004 (2020) 361–366, http://dx.doi.org/10.4028/www.scientific.net/msf.1004.361.

[28] G. Ristić, S. Golubović, M. Pejović, P-channel metal–oxide–semiconductor dosimeter fading dependencies on gate bias and oxide thickness, Appl. Phys. Lett. 66 (1995) 88–89, http://dx.doi.org/10.1063/1.114155.

[29] G.S. Ristic, Thermal and UV annealing of irradiated pMOS dosimetric transistors, J. Phys. D: Appl. Phys. 42 (2009) http://dx.doi.org/10.1088/0022-3727/42/13/135101, 135101–1–12.

[30] G.S. Ristić, N.D. Vasović, A.B. Jakšić, The fixed oxide traps modelling during isothermal and isochronal annealing of irradiated RADFETs, J. Phys. D: Appl. Phys. 45 (2012) http://dx.doi.org/10.1088/0022-3727/45/30/305101, 305101–1–11.

[31] G. Kramberger, K. Ambrožič, U. Gürer, B. Hiti, H. Karacali, I. Mandić, E. Yilmaz, O. Yilmaz, M. Zavrtanik, Development of MOS-FET dosimeters for use in high radiation fields, Nucl. Instrum. Methods Phys. Res. A 978 (2020) 164283, http://dx.doi.org/10.1016/j.nima.2020.164283.

[32] G.S. Ristic, M.S. Andjelkovic, R. Duane, A.J. Palma, A.B. Jaksic, Radiation and spontaneous annealing of radiation-sensitive field-effect transistors with gate oxide thicknesses of 400 and 1000 nm, Sensors Mater. 33 (6) (2021) 2109–2116, http://dx.doi.org/10.18494/SAM.2021.3425.